JOURNAL OF GUIDANCE, CONTROL, AND DYNAMICS
Vol. 33, No. 4, July–August 2010

Investigation into Pilot Perception and Control During Decrab Maneuvers in Simulated Flight

J. T. Beukers,* O. Stroosma,† D. M. Pool,‡ M. Mulder,§ and M. M. van Paassen¶
Delft University of Technology, 2629 HS Delft, The Netherlands

DOI: 10.2514/1.47774

An experiment was conducted in the SIMONA Research Simulator at Delft University of Technology to investigate the influence of sway, roll, and yaw motion cues on pilot performance, control, and motion perception during decrab maneuvers. In the experiment, six pilots were instructed to perform manual decrab maneuvers in heavy crosswind conditions with a Cessna Citation 500 model. The contributions of yaw, roll, and sway motion stimuli were varied such that their effects on objective measures and subjective ratings could be examined. The results of this experiment show that yaw motion had a positive influence on performance in terms of lateral touchdown distance from the runway centerline. Roll motion significantly decreased roll rate variations during decrab. High workload and the relatively low intensity of lateral motion cues led to the fact that pilots were unable to give consistent fidelity ratings. This result emphasizes the need for an objective and quantifiable method to determine motion fidelity for such maneuvers. Pilot models can possibly be used to further investigate the influence of different motion cues in these transient control tasks.

I. Introduction

FLIGHT simulators are important tools for both pilot training and research into aerospace systems. Most simulators consist of a cockpit replica, an outside visual system and a motion system that together provide cues to achieve simulated flight at a desired level of fidelity. Because of the restricted freedom of movement of a simulator, however, it is virtually impossible to provide exactly the same motion cues as in real flight. This induces a mismatch in stimuli compared with actual flight, which in turn causes pilots to adapt their control behavior, thereby limiting the simulator's fidelity and usefulness. Pilot models play an important role in gaining insight in this process [1–9].

In this light, a five-year research project was initiated at Delft University of Technology (TU Delft) to investigate simulator fidelity in more detail. The goal of this project is to develop a method to objectively and quantifiably assess the extent to which a flight simulator supports real-flight pilot behavior [10]. A cybernetic approach [11] is adopted that uses control-theoretical models to mathematically describe a pilot's multimodal response to visual and motion cues in real flight and in the simulator [12,13]. Currently, considerable experience has been gained by applying this approach to continuous control tasks, such as disturbance-rejection or target-tracking tasks, in which pilots manually control an aircraft relative to an equilibrium point [14–18].

Maneuvers that are essential ingredients of pilot training, however, are typically of a more *transient* nature and thus require transient rather than continuous pilot control inputs. In these transient control tasks, pilots bring the aircraft from one equilibrium state to another, such as in the case of an engine-out after takeoff, a helicopter deceleration to hover, or a decrab before landing in heavy crosswind.

Fundamental differences between continuous control tasks and these discrete transient maneuvers make the analysis of the latter much more complicated. First, these maneuvers are of relatively short duration compared with tracking tasks, which can last several minutes. As a result, the information per measurement is relatively low and maneuvers need to be repeated extensively to obtain reliable results. Second, pilot control behavior in continuous control tasks can be described with quasi-linear pilot models that can be identified from measured data using frequency- [19,20] and time-domain [21] identification techniques. Such linear models are not available for transient maneuvers. In addition, due to their short duration, frequency-domain identification techniques are not expected to yield satisfactory results when studying pilots' transient responses.

As a prelude to a cybernetic approach in which pilot control behavior is modeled for transient tasks, this paper describes a preliminary investigation into the influence of different motion stimuli on pilot behavior in transient maneuvers. The present study will form a basis for further investigation into the use of pilot models in describing and understanding transient control tasks. In this paper, a decrab maneuver before landing in heavy crosswind is considered. A decrab maneuver is almost always executed manually and, as it induces high pilot workload, requires extensive pilot training in simulators, making it a relevant maneuver to study. In addition, decrab maneuvers usually come with lateral acceleration profiles that are difficult to replicate with a reasonable level of fidelity in most hexapod simulators.

To examine the effects of lateral motion-cueing components on pilot perception and control, an experiment was performed in the SIMONA Research Simulator (SRS) of TU Delft. The experiment can be considered as a follow-up to the study performed by Smaili et al. [22], extending their experiment in a number of ways. First, to better represent the way a typical motion base is configured and tuned, a different work-space optimization method was chosen, as described in Sec. IV. In this method the lateral motion components were tuned for maximum work-space use in each experimental condition, rather than using constant filter gains that are tuned for one (full motion) condition only. Second, to allow for later comparison to real flight with TU Delft's laboratory aircraft, a Cessna Citation 500 aircraft model was used, which is considerably smaller than the Fokker 100 model used by Smaili et al. Third, additional performance and control metrics were used. Finally, only pilots actively

Presented as Paper 6030 at the AIAA Modeling and Simulation Technologies Conference, Chicago, IL, 10–13 August 2009; received 22 October 2009; revision received 2 February 2010; accepted for publication 3 February 2010.

*M.Sc. Student, Control and Simulation Division, Faculty of Aerospace Engineering; j.t.beukers@gmail.com.

†Researcher, Control and Simulation Division; o.stroosma@TUDelft.nl. Senior Member AIAA.

‡Ph.D. Candidate, Control and Simulation Division; d.m.pool@TUDelft.nl. Student member AIAA.

§Professor, Control and Simulation Division; m.mulder@TUDelft.nl. Senior Member AIAA.

¶Associate Professor, Control and Simulation Division; m.m.vanpaassen@TUDelft.nl. Member AIAA.

performing a decrab maneuver were considered in this paper, whereas in the research of Smaili et al., both pilots flying and pilots not flying were examined.

The paper is structured as follows. In the next section some general aspects of the decrab maneuver are discussed. In Sec. III, results from previous research regarding the effects of motion stimuli on pilot perception and control are summarized. Section IV describes the simulator motion cueing, including work-space optimization, used in the experiment. In Sec. V the experimental method is described, followed by Sec. VI, in which the results are presented. The results are discussed in Sec. VII and the paper ends with conclusions and recommendations.

II. Decrab Maneuver

A decrab maneuver is an asymmetric aircraft maneuver executed during final approach in crosswind conditions. Under such conditions, the initial approach is usually performed with wings level and with the nose of the aircraft pointed into the wind such that the aircraft approaches the runway slightly skewed, or crabbed, with respect to the runway. Figure 1a illustrates the aircraft attitude during initial approach in left crosswind conditions. Here, the aircraft flies with a compensating heading angle or crab angle ψ, such that the track angle χ (i.e., the heading of the ground speed vector) is aligned with the runway. Stick and pedals are in neutral position at this moment and wings are level.

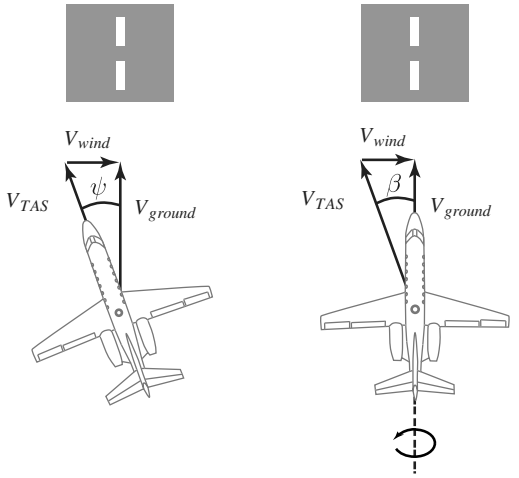

a) Before decrab maneuver **b) After decrab maneuver**

Fig. 1 Geometry of a left crosswind decrab maneuver.

To keep the lateral forces acting on the landing gear low when touching down, the pilot should ultimately align the aircraft with the runway. To achieve this, a decrab maneuver is generally performed using both aileron and rudder, with the desired outcome illustrated in Fig. 1b. Now the aircraft is lined up with the runway, inducing a sideslip angle β. Subsequently, roll correction is applied to prevent the aircraft from drifting sideways as a result of the slip angle. Lateral touchdown position and lateral velocity with respect to the runway are now controlled by carefully adjusting the aircraft roll attitude.

Decrabbing motion of an aircraft is characterized by roll and yaw rotations. In most aircraft the pilot station is located above and in front of the aircraft center of gravity and the rotations cause linear accelerations at the pilot station. The relation between the specific forces in the aircraft center of gravity $\bar{f}_{\text{cg}}$ and the specific forces at the pilot station, $\bar{f}_{\text{ps}}$ are given by

$$\bar{f}_{\text{ps}} = \bar{f}_{\text{cg}} + \dot{\bar{\omega}}_b \times \bar{r} + \bar{\omega}_b \times \bar{\omega}_b \times \bar{r} \tag{1}$$

where $\bar{\omega}_b$ is the aircraft body rate vector, and $\bar{r}$ is the spatial offset of the pilot station with respect to the center of rotation. In the Cessna Citation 500 aircraft, the pilot's head is located 3.2 m forward and 0.75 m above the center of gravity. As Eq. (1) indicates, the spatial offset can have a considerable influence on the specific forces during a decrab maneuver. Through dynamic coupling between both sideslip angle β and yaw rate r_b and roll rate p_b, the aircraft will also tend to roll when rudder inputs are given during a decrab maneuver. A representative motion profile obtained by using an autopilot in steady wind conditions is given in Fig. 2. Here, the lateral motion cues at the pilot head are shown in the time domain as well as in the frequency domain. In the frequency domain, the cues are compared with the vestibular thresholds for motion detection, as found by Heerspink et al. [23]. Note that the upper and lower thresholds as defined by Heerspink et al. are sensory thresholds, i.e., thresholds measured in the dark with single axis motion. During a decrab maneuver, the actual thresholds are expected to be higher, e.g., due to indifference effects from the combination of motion cues [24]. As such, these thresholds are not used here as a predictor of the motions' perceivability, but as a perception-based measure of motion magnitude.

From Fig. 2 it can be observed that the low-frequency parts of the sway specific force f_y and the roll acceleration are above absolute perception thresholds. Yaw cues, on the other hand, are found to be subthreshold for most runs. The influence of yaw motion cueing on perception ratings and performance can therefore be expected to be small, as will be further discussed in Sec. III.B.

The characteristic frequencies for the aircraft model in the landing configuration (including a yaw damper) as used in the experiment are given in Table 1. Both sway cues and roll cues at the Dutch roll

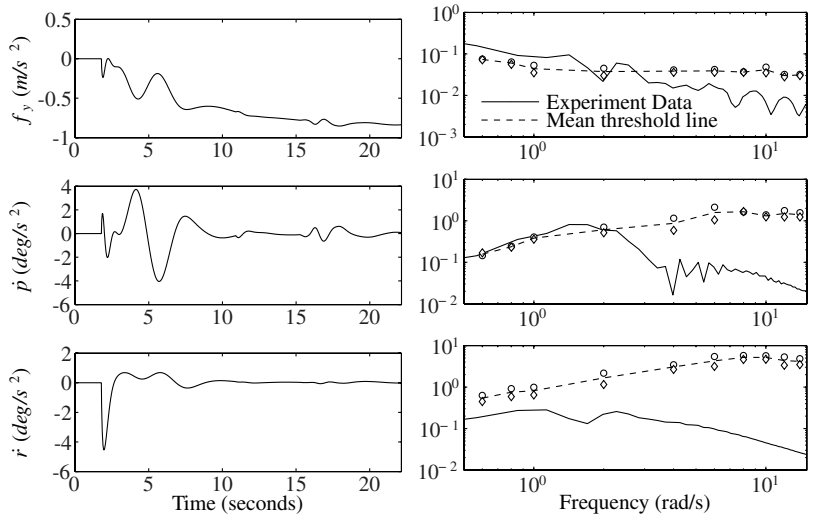

Fig. 2 Lateral motion cues at pilot head during an automated decrab maneuver compared with perception thresholds [23].

Table 1 Cessna Citation eigenmotions for experiment landing configuration

Eigenmotion	Eigenvalue λ	Natural freq. ω_0, rad/s	Damping ζ	Period P, s	Time to damp $T_{\frac{1}{2}}$, s
Short period	$-1.30 \pm 1.66j$	2.11	0.617	2.98	0.533
Phugoid	$-0.0251 \pm 0.221j$	0.223	0.113	28.2	27.6
Dutch roll	$-1.05 \pm 1.32j$	1.69	0.623	3.72	0.659
Spiral	0.0152	——	——	——	−45.7
Roll subsidence	−2.22	——	——	——	0.313

frequency, the dominant lateral mode, of 1.7 rad/s are expected to be perceivable during decrab maneuvers in the actual aircraft.

III. Previous Research

Presenting motion cues to a pilot in simulated flight has often been shown to increase pilot performance [18,25] and the pilots' subjective impressions of simulator fidelity [26]. A large variety of studies have been conducted on the influence of individual motion-cueing components on pilot control performance, pilot motion perception, and simulator fidelity ratings. A selection of studies that focused on lateral motion cueing and are thus of interest for aircraft decrab maneuvers are discussed here.

A. Helicopter Simulation Experiments

A series of experiments of particular interest to the current study were concerned with helicopter simulation. Schroeder [27] explored motion cueing on NASA's Vertical Motion Simulator in four of the six rigid-body degrees of freedom (roll, yaw, sway, and heave) for multiple helicopter control tasks, among which was a yaw capture task. He found that lateral and vertical translational motion platform cues had significant effects on reported simulator fidelity and pilot performance and that they reduced pilot physical and mental workload. Yaw and roll rotational motion platform cues were found to be less important. In particular, yaw rotational motion cues did not appear at all useful for improving performance or reducing workload. It was also concluded that combining lateral translational motion cues with visual yaw rotational cues could induce a sensation of physical rotation, even when the motion platform was not rotating.

Grant et al. [28] repeated the yaw capture task of the research of Schroeder [27] in the University of Toronto Institute for Aerospace Studies (UTIAS) Flight Research Simulator and focused on the roles of sway translation and yaw rotation. Again, translational motion was found to improve pilot performance. In contrast to the conclusions of Schroeder, Grant et al. [28] found that yaw motion could also increase performance, although additional improvements in the presence of translational motion were small. Both studies agreed on the fact that sway motion could be perceived as yaw motion when combining it with visual yaw rotational cues. Ellerbroek et al. [14] did a second repetition of Schroeder's [27] yaw capture experiment in the SRS at TU Delft and added a combined disturbance and tracking task to further examine the individual effects of yaw and sway motion cues. In contrast to the conclusions of the two previous experiments, it was found that yaw and sway motion showed more equal contributions to pilot performance and fidelity ratings. Although disagreement exists about the role of yaw, the significance of the effect of sway motion cues was demonstrated in all three studies.

B. Aircraft Decrab Simulation Experiments

A second series of experiments that are of interest to the research described in this paper, investigated decrab maneuvers in crosswind before landing. Groen et al. [29,30] examined the effects of sway, roll, and yaw on pilot perception for passive decrab maneuvers using the Generic Fighter Operations Research Cockpit Environment (GFORCE) of the National Aerospace Laboratory (NLR). A simplified and adapted Fokker 100 aircraft model was used in this study. The research concluded that subjective perception of motion during a decrab maneuver was dominated by sway and roll, rather than yaw. A remarkable result in this study was that 30% of the pilots still reported to sense motion in the condition *without* outside visual, even when the simulator was *not* moving. This indicates that pilots sometimes tend to perceive motion out of expectation, rather than perceiving it through their vestibular system.

In a follow-up study, Smaili et al. [22] examined the effects of sway, roll, and yaw on subjective pilot perception, simulator fidelity rating, pilot workload, and pilot compensation for both passive and active decrab maneuvers. In this research, a Fokker 100 aircraft model was simulated in the Generic Research Aircraft Cockpit Environment (GRACE) of the NLR. The results showed that reported perception of simulator motion was positively affected by platform sway for both the pilots flying and pilots not flying. The roll-only condition had a significant influence on motion perception for the pilots not flying. Platform yaw motion seemed to only have a positive effect on motion perception in the absence of sway. No significant effects on the fidelity ratings for pilots flying were found.

From these previous studies it can be concluded that in relatively simple control tasks such as a helicopter yaw capture task, sway motion cues are likely to improve pilot performance and simulator fidelity. For these tasks, the benefits of adding yaw and roll motion cues were shown to be not significant. For decrab maneuvers, sway can be expected to increase the perception of motion. No significant effects of lateral motion-cueing components on reported simulator fidelity were found.

IV. Simulator Motion Cueing

Pilot control behavior depends on the information available in the environment, perceived through a complex multisensory system with contributions from visual, vestibular, and proprioceptive sensors. This section will discuss the generation of simulator motion cues and the motion-cueing algorithm optimization process used in this study, which aimed at a fair comparison between motion configurations and an optimal use of the available simulator work space.

A. Classical Washout Algorithm

The limited work space available for flight simulator motion makes the generation of motion cues a challenging problem. To compensate for the inability to provide the exact same cues in a simulator as in a real aircraft, limitations in the human vestibular system are exploited as motion-cueing algorithms drive the motion system such that perceived differences between simulator motion and real aircraft motion are sufficiently small.

The most widely used motion drive algorithm in commercial simulators is the classical washout algorithm (CWA). First proposed by Schmidt and Conrad [31] and further improved and documented by Reid and Nahon [32,33], the CWA is characterized by the separation of high-frequency and low-frequency motion content using linear high-pass and low-pass filters. The underlying principle of the algorithm is that high-frequency accelerations and angular rates are able to pass through, but low-frequency components, the components that otherwise would induce large actuator displacements, are attenuated. Sustained longitudinal and lateral specific forces can be simulated by tilting the simulator cabin at subthreshold rates, such that gravitational components arise in the body reference frame. The effectiveness of the CWA was demonstrated in a study by Reid and Nahon [33]. In an analysis of the frequency response of this algorithm they showed that when neglecting scaling and limiting and further assuming small angles, the overall transfer function between

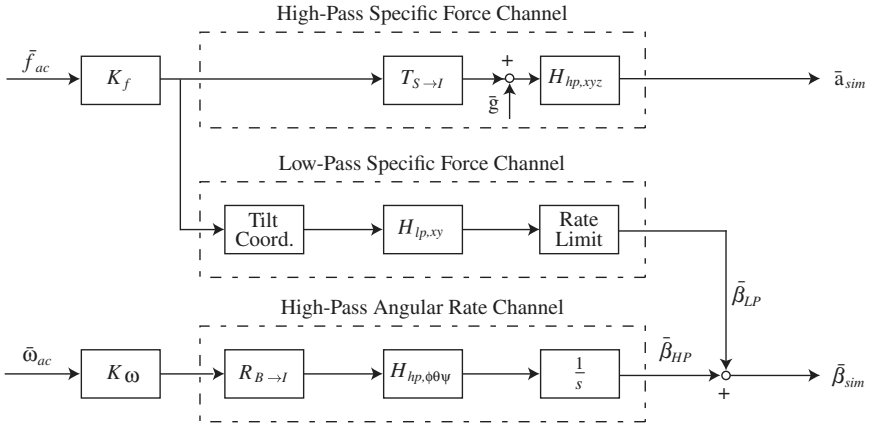

Fig. 3 Classical washout algorithm.

uncoordinated aircraft pitch or roll motion and the corresponding simulator motion was close to unity at all frequencies.

A schematic representation of the CWA is given in Fig. 3. All reference frames used in the definition of the CWA are defined in Appendix A of this paper. In Fig. 3, it can be seen that the inputs of the algorithm consist of specific forces $\bar{f}_{\text{ac}}$ and angular rates $\bar{\omega}_{b,\text{ac}}$ computed in the aircraft model. Note the similarity with the human vestibular system, which enables human perception of specific forces $\bar{f}$ through the otoliths and of angular rates $\bar{\omega}$ through the semicircular canals [34]. Before filtering, the input channels are scaled with filter gains $K_f = \text{diag}(K_{f_x}, K_{f_y}, K_{f_z})$ and $K_\omega = \text{diag}(K_{\omega_p}, K_{\omega_q}, K_{\omega_r})$ and transformed to the inertial reference frame by transformation matrices $T_{S\to I}$ and $R_{B\to I}$. Both matrices depend on the actual state of the simulator and are therefore continuously updated. After scaling and transformation to the inertial reference frame the specific forces and angular rates are high-pass filtered in the high-pass channels using $H_{\text{hp},xyz}$ and $H_{\text{hp},\phi\theta\psi}$, respectively. In the low-pass specific force channel, surge and sway specific forces are filtered by a low-pass filter $H_{\text{lp},xy}$ and then used to tilt the cabin. An implementation of the CWA is characterized by the combination of the selected filter gains and break frequencies.

For this study, the CWA was adapted to allow the enabling and disabling of individual degrees of freedom. For roll and yaw this was done by employing a zero gain at the input of the algorithm. For the sway degree of freedom a specific force input of zero would still lead to large sway movements in the presence of roll, as the simulator would try to negate the roll-induced specific force from gravity. This problem was solved by introducing a second scaling gain at the sway output of the algorithm, which could be set to zero when disabling the sway channel. As a result, the pilots could still perceive sway specific forces when sway was disabled, but these would only be caused by the simulator's roll angle and not by any lateral simulator accelerations.

A second adaptation to the CWA was the addition of prepositioning. With prepositioning, a larger part of the motion space can be used when the future maneuvers can be anticipated, as was the case in this study. During the initial part of the flight the simulator was smoothly repositioned in sway and heave with subthreshold accelerations [35]. The amount of prepositioning was determined as described in Sec. IV.C.1.

Table 2 Combinations of lateral motion-cueing components

Condition	Symbol	Sway	Roll	Yaw
No lateral motion	no	——	——	——
Yaw	y	——	——	×
Roll	r	——	×	——
Roll/yaw	ry	——	×	×
Sway	s	×	——	——
Sway/yaw	sy	×	——	×
Sway/roll	sr	×	×	——
Sway/ roll/yaw	sry	×	×	×

B. Experimental Conditions

As stated in the Introduction, the individual effects of lateral motion-cueing components on pilot perception and control will be examined in this paper. With three separate motion components under investigation, the eight possible combinations are defined in Table 2. It should be noted that longitudinal motion cueing (i.e., surge, heave, and pitch cueing) is present in all eight conditions as well, and their filter settings are kept constant for all conditions.

C. Motion Filter Tuning

Now that the structure of the motion drive algorithm has been defined, the CWA parameters for the different motion-cueing conditions can be determined. The values of these parameters have a large influence on the motion profile that is ultimately sensed by a pilot in the simulator [36]. A systematic tuning approach is therefore essential for a good simulator experiment.

In the research of Smaili et al. [22] the strategy was adopted to tune the motion filter settings such that optimal work-space use is guaranteed in the full motion condition. The other motion-cueing conditions were obtained by setting the appropriate filter gains to zero. A disadvantage of this tuning strategy, however, is the suboptimal (and thus less representative of real-world applications) use of the available motion space in conditions other than full motion. For this reason, another tuning strategy is adopted in this paper. First, filter gains and break frequencies were determined such that in the yaw-only (y), roll-only (r), and sway-only (s) conditions the simulator work space was used optimally. Second, the settings for the other conditions were obtained by reducing all lateral filter gains proportionally to keep the simulator within its work space. Motion filter break frequencies remained unchanged in this process. The advantage of this tuning strategy is that for each condition the simulator motion cueing makes full use of the available work space and the overall motion magnitude is comparable for all conditions.

To ensure limited simulator displacement through sufficient motion washout for the studied maneuver, in combination with minimal phase distortion, the high-pass and low-pass (tilt coordination) translational filters were of second order [Eqs. (2) and (3)] and the rotational filters were of first order [Eq. (4)]. The damping coefficients of all filters were set to unity:

$$H_{\text{hp},xyz}(s) = \frac{s^2}{s^2 + 2\zeta\omega_{n,\text{hp}}s + \omega_{n,\text{hp}}^2} \tag{2}$$

$$H_{\text{lp},xy}(s) = \frac{\omega_{n,\text{lp}}^2}{s^2 + 2\zeta\omega_{n,\text{lp}}s + \omega_{n,\text{lp}}^2} \tag{3}$$

$$H_{\text{hp},\phi\theta\psi}(s) = \frac{s}{s + \omega_{b,\text{hp}}} \tag{4}$$

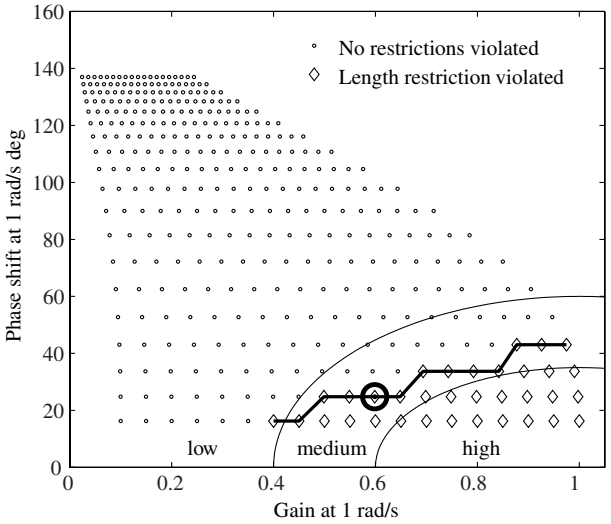

Fig. 4 Work-space boundary definition for SRS adjusting sway high-pass filter.

1. Lateral Motion Filter Tuning

The filter gains and break frequencies of the lateral motion channels were carefully tuned using the approach of Gouverneur et al. [37], which makes use of the Sinacori motion fidelity criterion [38], the later work of Schroeder [27], and offline estimates of the required actuator extensions. Characteristic motion profiles of various piloted decrab runs performed in the SRS during the testing phase of the experiment were used for this tuning.

In Fig. 4 the Sinacori motion fidelity criterion is shown for sway high-pass filter settings for the sway-only condition. In the figure, each point represents a filter with a unique combination of high-pass filter gain and break frequency. For a large number of combinations, the phase shift and system gain of the filter are calculated at a frequency of 1.0 rad/s and added to the Sinacori plot. In this figure, high system gain and low phase shift correspond with high motion fidelity [27]. Gouverneur et al. [37] proposed that for each combination of high-pass filter gain and break frequency, an assessment can be made whether the simulator actuators would violate an actuator length, velocity, or acceleration restriction for a particular motion profile. The Sinacori criterion in combination with the approach of Gouverneur et al. and a suitable reference profile can now provide guidance for choosing a combination of filter parameters that results in minimum phase shift and maximum system gain without violating actuator restrictions. For the actuator restrictions, an operational range of ± 0.555 m was used for the SRS. Furthermore, actuator velocity was restricted at 1 m/s and actuator acceleration was restricted at 10 m/s^2 [37]. For this experiment, the actuator length was found to be the primary restriction.

From Fig. 4 the encircled point was chosen as an optimal combination of low phase shift and relatively high system gain at which the actuator length criterion was only just violated. This point corresponded to a system gain of 0.59 and a phase shift of 24.78° for a 1.0 rad/s input signal. The corresponding sway high-pass filter had a filter gain K_{f_y} of 0.6 and a break frequency ω_{n,hp_y} of 0.3 rad/s. The low-pass break frequency was defined relative to the high-pass break frequency as recommended by Reid and Nahon [33] for a good transient response to a step change in specific force $\bar{f}_{\mathrm{ac}}$:

$$\omega_{n,\mathrm{lp}} = 2\omega_{n,\mathrm{hp}} \tag{5}$$

New offline simulations were performed with these filter parameters to examine the actuator extensions with respect to their minimum and maximum strokes. An example of the actuator extensions for the sway-only condition is given in Fig. 5a. A definition of the actuator designations is given in Appendix A of this paper.

From Fig. 5a it can be observed that without prepositioning, the first and fourth actuators would violate their maximum extensions due to the large lateral displacement of the simulator cabin. This was,

Table 3 Proportional scaling for motion-cueing combinations

Condition	K_p
Roll/yaw	0.4
Sway/yaw	0.9
Sway/roll	0.4
Sway/roll/yaw	0.4

Table 4 Lateral motion filter settings

Parameter	no	y	r	ry	s	sy	sr	sry
K_p	——	1.0	1.0	0.4	1.0	0.9	0.4	0.4
Sway								
K_{f_y}	——	——	——	——	0.60	0.54	0.24	0.24
ω_{n,hp_y}, rad/s	——	——	——	——	0.30	0.30	0.30	0.30
ω_{n,lp_y}, rad/s	——	——	——	——	0.60	0.60	0.60	0.60
Roll								
K_{ω_p}	——	——	0.80	0.32	——	——	0.32	0.32
ω_{b,hp_p}, rad/s	——	——	0.30	0.30	——	——	0.30	0.30
Yaw								
K_{ω_r}	——	1.00	——	0.40	——	0.90	——	0.40
ω_{b,hp_r}, rad/s	——	0.05	——	0.05	——	0.05	——	0.05
y_{pp}, m	——	——	——	——	0.5	0.45	——	——
z_{pp}, m	——	——	0.1	0.1	0.1	0.1	0.1	0.1

Table 5 Longitudinal motion filter settings

Channel	K	$\omega_{n,\mathrm{hp}}$, rad/s	$\omega_{n,\mathrm{lp}}$, rad/s	$\omega_{b,\mathrm{hp}}$, rad/s
Surge	0.60	2.00	4.00	——
Heave	0.60	2.00	——	——
Pitch	0.45	——	——	0.25

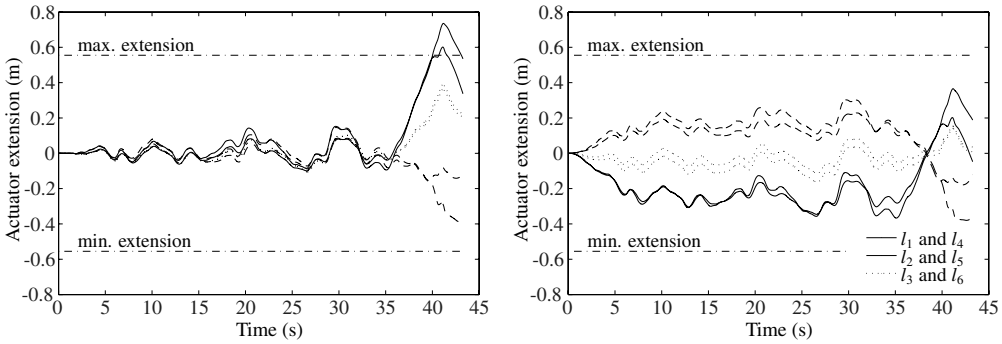

a) Actuator lengths for decrab without prepositioning **b) Actuator lengths for decrab with prepositioning**

Fig. 5 Actuator extensions for an experimental decrab run for $K_y = 0.6$ and $\omega_{n,\mathrm{hp}_y} = 0.3$ rad/s, sway-only condition. Final prepositioning is $y_{\mathrm{pp}} = 0.5$ m and $z_{\mathrm{pp}} = 0.1$ m.

of course, expected because of the length violation found in Fig. 4. By applying a prepositioning y_{pp} of 50 cm in the sway direction, an actuator profile with a buffer of 20 cm at both sides was obtained (Fig. 5b). This buffer of 20 cm at both sides was used for all conditions to account for different piloting techniques. Furthermore, a prepositioning z_{pp} of 10 cm in the downward heave direction also showed to improve the use of work space for this condition.

This two-stage design approach using the Sinacori fidelity criterion and the evaluation of the actuator extensions was performed for the yaw-only, roll-only, and sway-only conditions. For each of the other conditions, the first stage of selecting the break frequency and gain was replaced by the selection of a proportional gain K_p, which uniformly restricts the gains on all lateral degrees of freedom relative to the singular motion conditions. Any required prepositioning was then chosen by examining the actuator extension plots. Table 3 lists the resulting scaling factors. The filter parameters for the lateral channels that were ultimately obtained are summarized in Table 4.

2. *Longitudinal Motion Filter Tuning*

The filter gains and break frequencies of the longitudinal motion channels (surge, heave, and pitch) were taken equal for all eight conditions. For the longitudinal translational cues to have little influence on the use of simulator work space during the experiment, high-pass break frequencies for the second-order surge and heave filters, ω_{n,hp_x} and ω_{n,hp_z}, respectively, were chosen relatively high at 2 rad/s, similar to those used by Smaili et al. [22]. The low-pass break frequencies were chosen according to Eq. (5). Pitch rotation filter gain K_{ω_q} and break frequency ω_{b,hp_q} were chosen equal to the values of the experiment of Smaili et al. [22]. To conclude the definition of the filter parameters for the longitudinal channels, surge filter gain K_{f_x} and heave filter gain K_{f_z} were taken equal to the nominal sway filter gain K_{f_y} (i.e., 0.6) from Sec. IV.C.1. The longitudinal filter settings are summarized in Table 5.

V. Experiment

To further investigate the mixed results found in literature for the influence of yaw and roll rotational and sway translational motion on pilot perception and control performance in decrab maneuvers, an experiment was designed comparable with that of Smaili et al. [22]. For the experiment, pilots were asked to perform a large number of decrab maneuvers. This section describes important aspects of the setup of this experiment, in addition to the definition of the motion cueing already provided in Sec. IV.

A. Apparatus

The experiment was conducted in the SIMONA Research Simulator (Fig. 6) [39] of TU Delft. The SRS is equipped with a $180^\circ \times 40^\circ$ collimated visual display system with a refresh rate of 60 Hz. Dynamics of the visual system can be regarded as a pure time delay τ_v, which was shown to have an average value of approximately 25–30 ms [14]. The dynamics of the SRS motion system can be described by a second-order low-pass filter multiplied with a pure delay τ_m of approximately 30 ms [40]. The interior of the cabin is outfitted as a generic two-person cockpit of a modern airliner. The pilots controlled the aircraft from the left-hand seat, which was fitted with a loaded control column and rudder pedals. The dynamic characteristics of the controls were matched to the aircraft as much as possible. Furthermore, an inertial measurement unit was installed near the simulator's motion reference point, such that the actual specific forces and rotational accelerations in the simulator were known.

B. Task

To concentrate on the execution of the decrab maneuver itself, each experimental run was initiated on final approach at a radio altitude of 350 ft to land on runway 06 of Amsterdam Airport Schiphol (EHAM). At the start of a run the aircraft was trimmed in the landing configuration on the glide slope for a steady instrument-landing-system approach. Indicated airspeed was 110 kt and aircraft weight was 11,000 lb. Visual-flight-rules conditions were applicable and a realistic view out of the window was presented. Crosswind of 20 kt was present perpendicular to the runway from either left or right, resulting in a crab angle of 10.5°.

Pilots were asked to decrab the aircraft at a height of their choice, such that touchdown would take place with minimum lateral velocity and lateral offset with respect to the runway centerline and minimum heading-angle error. Thresholds for these measures were defined at 1 m/s lateral velocity, 5 m lateral offset, and 5 deg heading error. When exceeding any of these thresholds, performance was defined to be inadequate and the run was discarded and repeated. The run ended at 3 s after touchdown, such that the experimental scenario covered the entire landing phase. Because the aircraft model lacked lateral gear dynamics, the aircraft could slide somewhat after touchdown and the pilots were instructed to ignore the rollout motions just before simulator freeze.

To increase the feeling for the aircraft dynamics and to add some workload in the approach before decrab, turbulence was added based on the patchy model developed by Van de Moesdijk [41]. For the turbulence to have relatively little influence on motion cueing and control during decrab and to increase repeatability of the turbulence realization, the symmetrical deviations from the Gaussian distribution function were kept small.

C. Participants and Instructions

Six experienced Cessna Citation II pilots participated in the experiment. The participants, all males, had an average age of 51 years ($\sigma = \pm 14.8$ years) and had an average flying experience of 7800 h ($\sigma = \pm 4200$ h). Participants were elaborately briefed before the experiment and when extra instruction proved to be necessary, it was given during the training period. The participants were instructed to make a landing with heading alignment, lateral offset from the runway centerline, and lateral velocity as small as possible. No instructions were given regarding the longitudinal touchdown position or the vertical speed at touchdown.

a) SRS with its hexapod motion base **b) SRS flight-deck and outside visual**

Fig. 6 SIMONA Research Simulator.

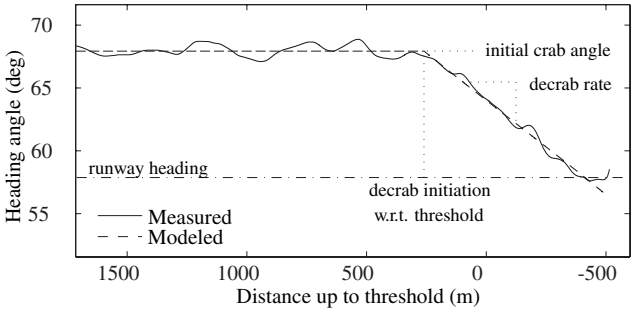

Fig. 7 Model definition for determining decrab initiation and decrab rate (w.r.t. means with respect to).

D. Aircraft Dynamic Model

The DASMAT nonlinear Cessna Citation 500 aircraft model, as documented by Van der Linden [42], was used in this study. This aircraft is a relatively lightweight twin-engine type and is smaller in length (13.26 m) than the Fokker 100 model (35.53 m) used in the work of Groen et al. [29,30] and Smaili et al. [22]. Sway cues due to yawing were therefore somewhat smaller, but rotational cues were expected to be larger than for the Fokker 100. Given the fact that most disagreement exists in the literature about the role of yaw and roll in simulator fidelity, this could be advantageous for the purposes of the experiment. Furthermore, a Cessna Citation model was chosen such that experiment results could eventually be compared with real flight data using the laboratory aircraft of TU Delft, a Cessna Citation II. Table 1 already gave an overview of the dynamic characteristics of the used aircraft configuration.

E. Independent Variables

As discussed in Sec. IV.C, a motion filter tuning strategy was adopted that strived for full use of the available simulator work space. The use of simulator work space turned out to be similar for each motion condition, with the exception of the no-lateral motion condition (no) and the yaw condition, the latter due to the simulator's ability to comfortably present full yaw motion well within the work space [35]. It was therefore assumed that the three motion components were independent, as their presence or absence had no influence on the use of simulator work space and the overall magnitude of motion cues. For the statistical analysis of the results it was assumed that the experiment had three independent variables (yaw, roll, and sway), which could be either absent or present.

The experiment was defined as a within-subject or repeated-measures design, meaning that each participant evaluated all conditions. In addition, the wind direction was varied between left and right during the experiment, but the effects of wind on the dependent measures were not analyzed. To diminish the influence of wind on the results, each block of eight conditions was combined with a random permutation of the four right and four left crosswind conditions, such that both wind directions were presented the same number of times.

F. Experiment Design and Procedure

The experiment was conducted in three phases: one block of 24 training runs and two blocks of each 16 experiment runs. A run lasted up to 3 s after touchdown, which resulted in an average runtime of 45 s. Data were recorded at 100 Hz. During training, pilots got accustomed to the simulator environment, the aircraft dynamics, and the experimental procedure. During the experiment phase each condition was repeated four times. The order in which the conditions were presented was randomized, such that the different conditions were distributed evenly over the participants and such that fatigue would not lead to unwanted systematic variance in the results.

G. Dependent Measures

In this experiment the influence of the independent variables on pilot performance, control activity, pilot perception, and simulator fidelity was examined, using both objective and subjective measures. Various dependent measures were identified to quantify these concepts.

1. Objective Measures

Pilot performance was determined by three groups of dependent measures. A first group of measures focused on the aircraft state at touchdown. Here, the lateral velocity and lateral position with respect to the runway centerline and the heading alignment were considered. Furthermore, although not a part of the instructions, the position with respect to the runway threshold and the vertical velocity were also considered at touchdown. In a second group of measures, the entire decrab phase was analyzed. The root mean square (RMS) was calculated for the localizer error and the roll rate. A third group of performance measures consisted of the maximum yaw rate, the minimum crab angle, the point of decrab initiation, and the average decrab rate.

For the calculation of the RMS of certain signals, a window was defined in which every decrab maneuver could be captured. When only considering the data within this window, the data during the crabbed approach were neglected, while still being able to compare results independently. The window was defined by means of distance with respect to the runway threshold, and the boundaries were set to include flights with both high and low decrab rates. The window ran from 200 m in front of and 450 behind the threshold.

For the calculation of the position of decrab initiation relative to the runway threshold and the average decrab rate, the model illustrated in Fig. 7 was used. A least-squares procedure was used to determine the model's parameters: the initial crab angle, the decrab initiation point, and the decrab rate.

Control activity was examined using four dependent measures. First, the RMS of the pedal rate and the wheel rate were determined during the decrab. Here, control *rates* were preferred over control *deflections,* since the nature of decrab control would result in nonzero

Table 6 Intensity rating scale

Ordinal	Label	Description
0.	No motion	No lateral motion cues were perceived in the simulator
1.	Too weak	Intensity of perceived lateral motion was too weak compared with expected motion cues
2.	Natural	Intensity of perceived lateral motion was natural compared with expected motion cues
3.	Too strong	Intensity of perceived lateral motion was too strong compared with expected motion cues

Table 7 Fidelity rating scale

Ordinal	Label	Description
0.	Low fidelity	Lateral motion-cueing differences from actual flight were noticeable and objectionable
1.	Medium fidelity	Lateral motion-cueing differences from actual flight were noticeable, but not objectionable
2.	High fidelity	Lateral motion cues were close to those of actual flight

mean deflection signals for both pedal and wheel and the RMS would not be suited for these kind of signals. Second, the maximum pedal deflection was determined, and third, the pedal deflection was integrated over time within the decrab window.

2. Subjective Measures

Finally, subjective measures for this experiment were considered, i.e., a rating for motion intensity and a rating for motion fidelity. The subjective measure of motion intensity was based on a four-point scale, given in Table 6, similar to the scale used by Smaili et al. [22]. The subjective measure of motion fidelity was based on a three-point scale, given in Table 7, also similar to that of Smaili et al. Note, however, that the verbal description for each point on the scale was added for this experiment specifically and was not used in the experiment of Smaili et al. Furthermore, note that the original scale descriptions were in Dutch, the native language of all participants.

H. Experiment Hypotheses

Previous research, summarized in Sec. III, generally indicated that sway cues had a larger positive influence on pilot performance and subjective fidelity than did roll and yaw cues. Although sway cues were expected to be relatively small in this study due to the chosen aircraft type, the same hypothesis is put forward here. Second, it is hypothesized that sway and roll cues increase motion intensity ratings. For motion intensity ratings, Smaili et al. [22] only found a significant influence of roll motion cues for the pilots not flying. However, since a smaller aircraft was used, the hypothesis was formulated that the role of roll cues would be larger. Third, it was hypothesized that yaw cues were below threshold and would therefore have no influence on the dependent measures.

VI. Results

The results of the experiment are presented in this section and the effects of the experimental conditions, as summarized in Table 2, on the dependent measures will be discussed. First, however, some general findings of the experiment will be discussed.

A. Decrab Variation

To produce consistent results that can form a solid foundation for later modeling efforts, the experiment would benefit from a constant decrab technique that is employed equally by all participants. This section examines the variation in piloting techniques and strategies employed in the experiment. First, to show the spread in touchdown positions during the experiment, some results of randomly chosen runs are shown in Fig. 8. An indication of the lateral velocity with respect to the runway centerline is given by the length of the vertical lines attached to each touchdown point. Longitudinal spacing of the touchdown points is shown to be considerable, but this is somewhat expected, since no instructions were given to the pilot concerning the longitudinal position of touchdown.

Second, to get an idea of the different strategies adopted by the pilots, the estimation results for decrab initiation and decrab rates from the model of Fig. 7 are plotted in Fig. 9. The data set is fitted to an exponential function using a least-squares method to show the correlation in the figure. The resulting correlation coefficient corresponding to this fit was 0.762. It can be seen that the execution of the decrab maneuvers had considerable variation over the different runs and that a strong correlation exists between decrab initiation and decrab rate, which could be expected. Some decrab maneuvers were executed quite gently over a longer period of time, while others were executed more fiercely in a matter of seconds. Section VI.B.3 further examines the influence of the different motion conditions on these parameters.

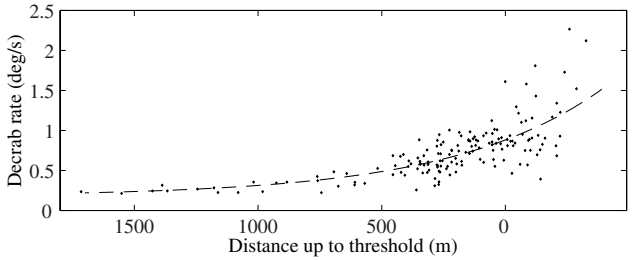

Fig. 9 Decrab initiation versus decrab rate for all experimental runs.

B. Pilot Performance

The effects of the motion filter settings on pilot performance will be discussed for the three groups of measures identified in Sec. V.G.1: the performance at touchdown, the performance during the decrab phase, and other characteristics of the decrab maneuver. All performance measures presented were adjusted for between-subject variability and tested for the normality assumption using a Kolmogorov–Smirnov test. Furthermore, the sphericity assumption for the data was tested with Mauchly's test. Ultimately, the significance of the effects of motion filter settings on the dependent measures was determined using a repeated-measures analysis of variance (ANOVA) with three independent variables, as described in Sec. V.E. In the analysis, a significance level of $p < 0.05$ will be used, and $p < 0.1$ will be regarded as a marginally significant result.

1. Performance at Touchdown

The performance measures that are examined here are lateral velocity, lateral distance from the runway centerline, heading alignment, vertical velocity, and the longitudinal distance from the runway threshold. All measures were determined per run at the moment of touchdown.

First, the results for lateral velocity are given in Fig. 10a. It is shown that the mean lateral velocity at touchdown was reasonably low, i.e., well below the set threshold value of 1.0 m/s, in all conditions. As indicated by the grouped results at the right of Fig. 10a, only roll had a marginally significant effect on this measure ($F_{1,5} = 5.750$, $p = 0.062$), with the addition of roll motion actually increasing lateral velocity at touchdown. Next, in Fig. 10b the lateral distance with respect to the runway centerline is given. As could already be expected from Fig. 8, the mean touchdown points were all well within the set boundary of 5 m. Here, rather surprisingly, a

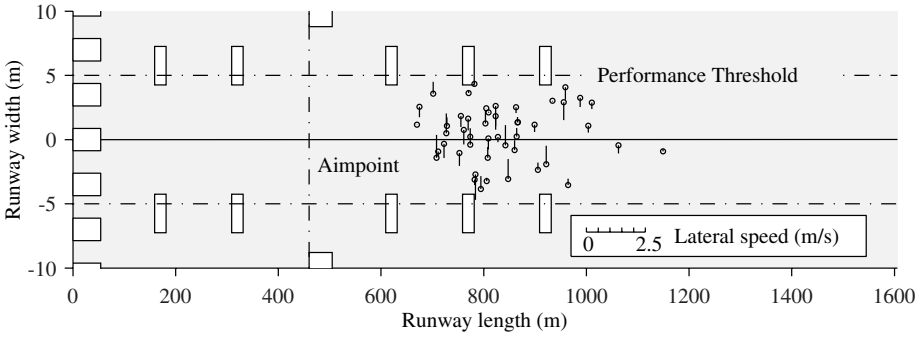

Fig. 8 Position and indication of lateral velocity at touchdown for a number of experimental runs.

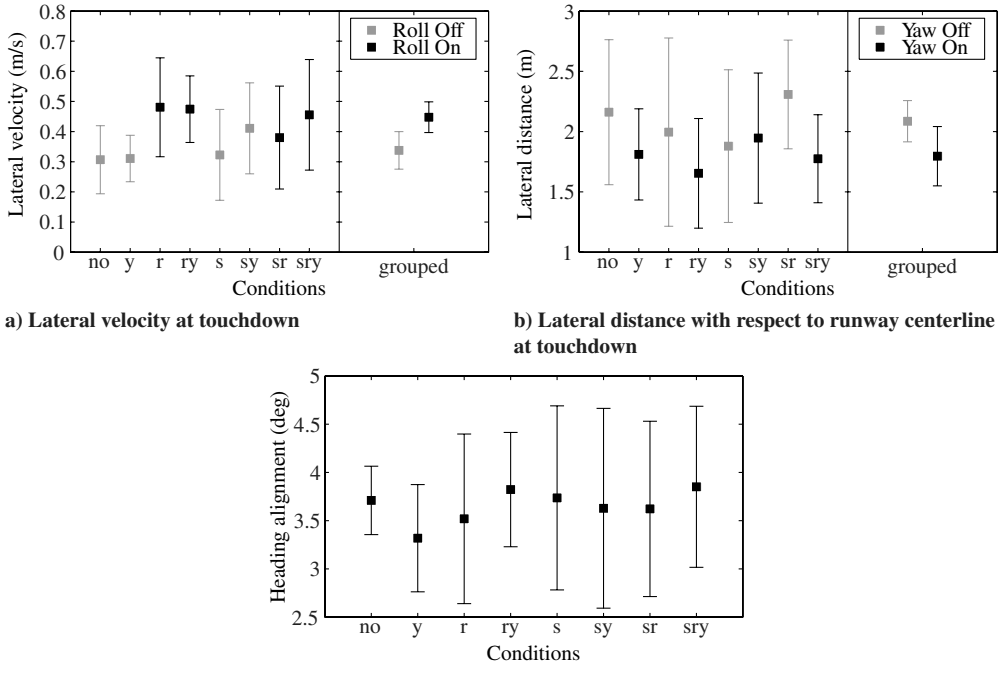

a) Lateral velocity at touchdown

b) Lateral distance with respect to runway centerline at touchdown

c) Heading alignment at touchdown

Fig. 10 Means and 95% confidence intervals of lateral velocity, lateral distance, and heading alignment at touchdown.

significant effect was found for the influence of yaw ($F_{1,5} = 9.431$, $p = 0.028$).

As a final lateral touchdown performance measure, the heading alignment at touchdown was considered. The results are shown in Fig. 10c. First, it can be observed that the pilots seldom performed a full decrab and retained some crab angle at touchdown. Furthermore, the differences of the heading alignment at touchdown for the different motion conditions are very small. The ANOVA showed no significant effects for this measure.

Although no instructions were given to the pilot considering the longitudinal position or the vertical velocity at touchdown, it is interesting to examine possible effects of the motion-cueing conditions on these quantities. The longitudinal distance, for example, can be assumed to be correlated with the difficulty of handling the aircraft. In Fig. 11 the mean values are given with their 95% confidence intervals.

By inspection, the trends in the two figures show resemblance, which is an indication of a correlation between touchdown position and vertical velocity, i.e., the earlier the touchdown took place, the harder the landing. A correlation coefficient $r = 0.682$ was found for these two measures with a significance level of $p = 0.062$ using Pearson's correlation analysis. In the ANOVA, a significant

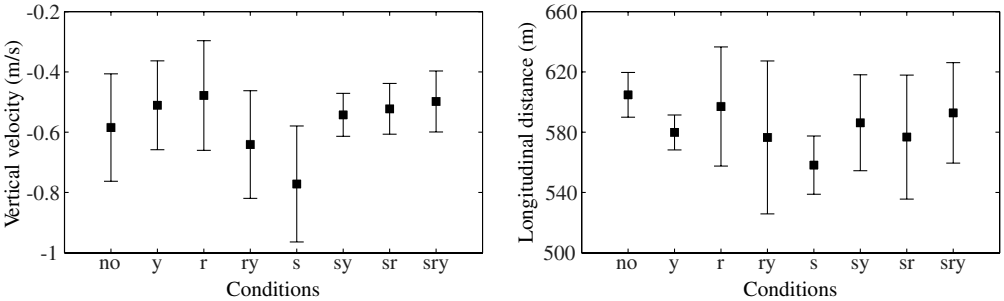

a) Vertical velocity at touchdown

b) Touchdown distance w.r.t. the runway threshold

Fig. 11 Means and 95% confidence intervals of vertical velocity and longitudinal distance at touchdown.

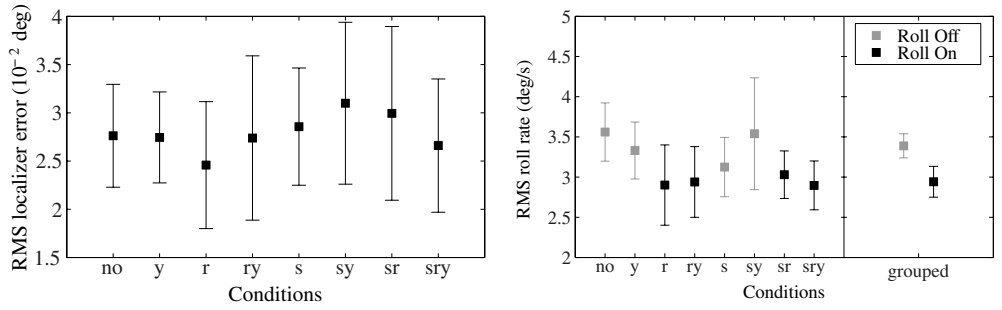

a) RMS localizer error

b) RMS roll rate

Fig. 12 Means and 95% confidence intervals of RMS of localizer error and roll rate within decrab window.

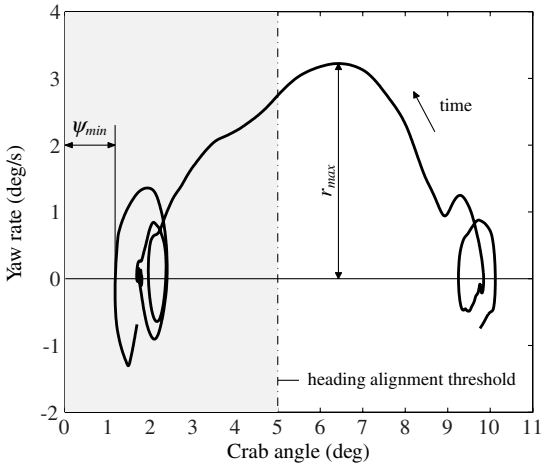

Fig. 13 Phase-plane portrait of a decrab run.

interaction was found between sway and yaw for the vertical velocity at touchdown ($F_{1,5} = 7.008$, $p = 0.046$). The same interaction shows a marginally significant effect on longitudinal distance ($F_{1,5} = 4.441$, $p = 0.089$). Marginally significant interactions were found for vertical touchdown velocity between yaw and roll ($F_{1,5} = 4.578$,$p = 0.085$) and between sway and roll ($F_{1,5} = 4.122$, $p = 0.098$).

2. *Decrab Performance*

Decrab performance should not only be determined at touchdown, but also during the maneuvering period. For this analysis, the mean values of the RMS of the localizer error and the RMS of the roll rate are considered. The starting and end points of both the localizer error and the roll rate are determined by the decrab window defined in Sec. V.G.1. In Fig. 12 the mean values for both measures are given together with their 95% confidence intervals.

No significant effects were found for effects of motion cueing on the RMS of the localizer error. The RMS of the roll rate during the decrab window, however, showed to be significantly dependent on roll motion cues ($F_{1,5} = 11.797$, $p = 0.019$). Roll rate significantly reduced when roll motion cues were presented. Some pilots reported small pilot-induced roll oscillations in conditions in which simulator roll motion was absent; this effect may be related to this reduced roll rate effect found in the statistical analysis.

3. *Other Performance Measures*

A third group of performance measures that could characterize a decrab maneuver was considered. First, the maximum yaw rate and minimum crab angle during the decrab phase were obtained for each run. Second, the model of Fig. 7 was fitted on the data of each run, such that the point of decrab initiation with respect to the runway threshold and the average decrab rate could be estimated.

Figure 13 shows a phase-plane portrait of a typical decrab run, in which crab angle and yaw rate can directly be compared. In this phase-plane portrait, the maximum yaw rate $r_{\max}$ and minimum crab angle can easily be observed. Note that when a heading overshoot took place, the minimum crab angle was defined as negative. It is remarked here that since yaw rate peaks could possibly also be induced by turbulence gusts, the causes of the maximum yaw rate values were first investigated. It was found that each yaw rate peak was indeed the result of the decrab motion.

The influence of motion-cueing conditions on the maximum yaw rate and the minimum crab angle are given in Fig. 14. Pearson's correlation coefficient $r = 0.235$ was found between maximum yaw rate and average decrab rate. However, the result was not significant ($p = 0.576$). No significant effects of the motion filter settings on the minimum crab angle were found as well. For the maximum yaw rate, however, a significant effect was found for the interaction of roll and yaw ($F_{1,5} = 27.527$, $p = 0.003$) and marginally significant reductions were observed for yaw ($F_{1,5} = 4.268$, $p = 0.094$) and sway ($F_{1,5} = 5.028$, $p = 0.075$).

The influence of motion-cueing conditions on decrab initiation and decrab rate was analyzed next, depicted in Fig. 15. Because of a violation of the normality assumption for both data sets, nonparametric Friedman's ANOVA was used for these measures. No significant effect of the motion-cueing settings on one of these two measures was found, however. Furthermore, Pearson's correlation analysis was performed to a show a possible correlation between the point of decrab initiation relative to the runway threshold

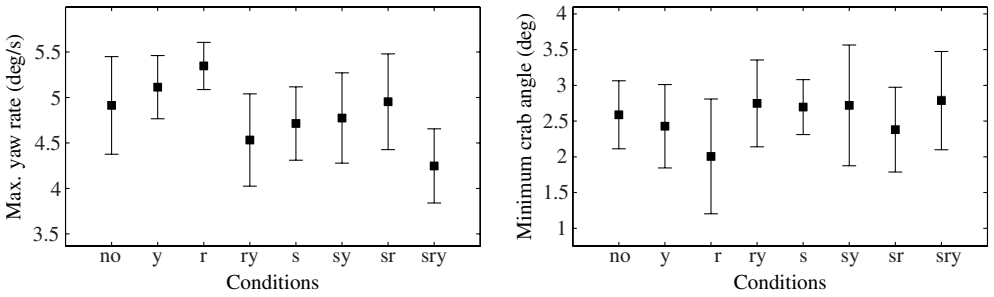

a) Maximum yaw rate **b) Minimum crab angle**

Fig. 14 Means and 95% confidence intervals of the maximum yaw rate and minimum crab angle.

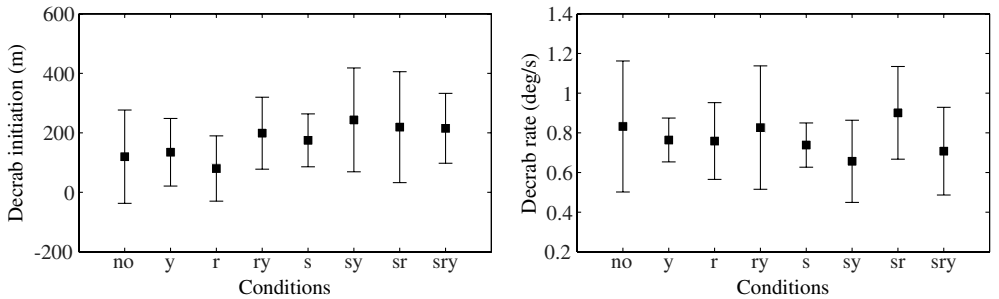

a) Decrab initiation w.r.t. runway threshold **b) Average decrab rate**

Fig. 15 Means and 95% confidence intervals of the point of decrab initiation w.r.t. the runway threshold and the average decrab rate.

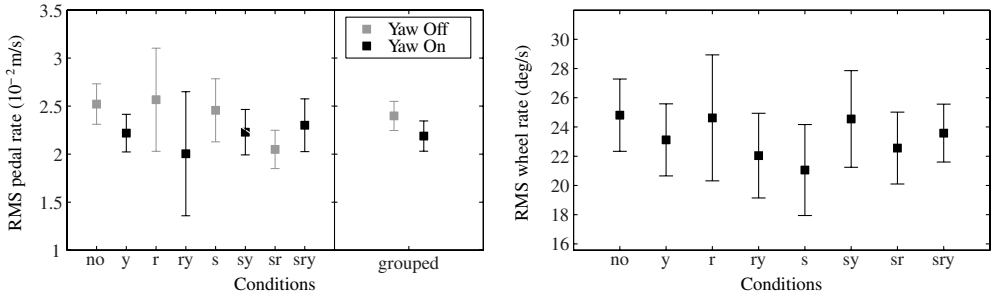

a) RMS of pedal rate b) RMS of wheel rate

Fig. 16 Means and 95% confidence intervals of RMS wheel rate and pedal rate within decrab window.

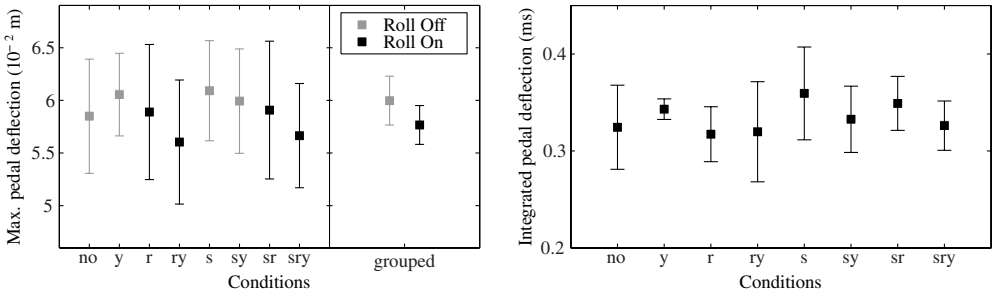

a) Maximum pedal deflection b) Integrated pedal signal

Fig. 17 Means and 95% confidence intervals of maximum pedal deflection and integrated pedal signal within decrab window.

and the average decrab rate. A correlation coefficient $r = -0.170$ was found, corresponding with an inverse correlation, but this result was not significant ($p = 0.688$).

C. Control Activity

The control activity of the pilots in the different motion conditions are examined by means of several control measures. The mean RMS values of the pedal and wheel rates, as well as the pedal deflection integrated over time, are examined within the decrab window. The maximum pedal deflection is also considered.

Mean RMS values of the pedal and wheel rate are given in Fig. 16 together with their 95% confidence intervals. Pedal control activity was slightly lower in the presence of yaw, but this effect was only marginally significant ($F_{1,5} = 6.564$, $p = 0.051$). It could be expected that wheel control activity was influenced by roll motion cueing, but this influence was not found ($F_{1,5} = 0.038$, $p = 0.852$). A significant interaction between yaw and sway was present in the data ($F_{1,5} = 8.639$, $p = 0.032$). The wheel rate RMS increased with the addition of sway when yaw was also present, but decreased without yaw.

The mean values for the maximum pedal deflection and the integrated pedal signal, the latter within the decrab window, together with their 95% confidence intervals are given in Fig. 17. The ANOVA showed that the effect of roll motion on maximum pedal deflection was marginally significant ($F_{1,5} = 4.274$, $p = 0.094$). The results also show that the interaction of sway and yaw had a significant effect on the integrated pedal signal ($F_{1,5} = 16.863$, $p = 0.009$). The pedal deflection slightly decreased with the addition of sway when yaw was also present, but increased without yaw. This is the opposite effect from that observed for the wheel rate RMS.

D. Subjective Ratings

In addition to the analysis of objective measures for pilot performance and control activity, subjective ratings for motion perception and simulator fidelity were examined. Note that unlike the objective measures, the ratings were not corrected for between-subject variability. First, the participants were asked to rate the motion intensity on the four-point scale of Table 6. Box plots of the mean ratings per pilot are given for each condition in Fig. 18a. The figure shows the median value, with boxes extending to the 25th and 75th percentile and whiskers containing the maximum and minimum values, unless there are outliers outside 1.5 times the interquartile range from the edge of the boxes. These outliers are displayed as a +. Note that this four-point rating scale is clearly

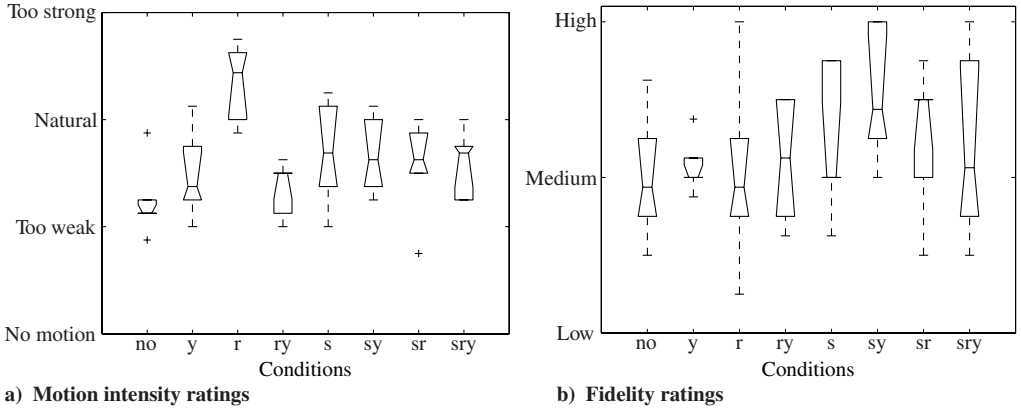

a) Motion intensity ratings b) Fidelity ratings

Fig. 18 Motion intensity and fidelity ratings (see Tables 6 and 7 for rating-scale definition).

ordinal, in contrast with the interval scale of the dependent measures discussed before. Since interval data is one of the assumptions for parametric tests, the repeated-measures ANOVA was not applicable here. Nonparametric Friedman's ANOVA was used instead to examine possible overall significant effects, and in the case of a significant result, Wilcoxon signed-rank post hoc tests were used for pairwise comparison between conditions.

From inspection, the lateral motion intensity in the roll-only condition was perceived as too strong. Furthermore, the four sway conditions appear to lead to higher ratings than in the no-motion, yaw-only, and roll/yaw (ry) conditions. Friedman's ANOVA showed a significant overall effect [$\chi^2(7) = 20.352$, $p = 0.005$]. As could be expected, the Wilcoxon signed-rank post hoc tests showed that this effect was mainly caused by the relatively high ratings for the roll-only condition. All pairs that included this roll-only condition showed to be significantly different, with significance levels between $p = 0.026$ (for the roll-only condition versus the no-motion condition) and $p = 0.046$ (for the roll-only condition versus the sway-only condition). One more significant result was found for the comparison between the no-motion condition and the sway-only condition ($p = 0.027$).

For the rating of simulator fidelity, the participants were asked to use the three-point scale of Table 7. Box plots of the mean ratings per pilot are given for each condition in Fig. 18b. The results show that the variance in the ratings is very high. From inspection, the combination of sway and yaw seems to have a positive influence on fidelity ratings. Although the sway conditions showed a slightly higher mean for the fidelity ratings, no significant overall effect was found using Friedman's ANOVA. Also note the very large variation in the fidelity ratings in the roll-only condition.

VII. Discussion

In general, the effects of varying lateral motion cueing on pilot behavior and motion fidelity ratings were found to be small for the decrab maneuver studied in this paper. This can be partially explained by the relatively small number of participants, but another aspect may be the particular motions the pilots experienced in the different conditions. To increase insight and perhaps allow for interpretation of some of the results, a selection of time histories of perceived lateral specific forces and roll rotational accelerations in different motion conditions is given in Fig. 19. Here, the aircraft model cues correspond with the cues that a pilot would perceive, i.e., rotational rates and specific forces at the pilot head, when actually flying in the aircraft. In contrast, the simulator cues correspond with the cues provided in the simulator during the experiment. The moment of decrab initiation, approximated with the model of Fig. 7, is given in these figures as well.

From Fig. 19 the effects of the filter settings for different motion-cueing conditions are evident. A low break frequency and a high filter gain resulted in a high correlation between simulator and aircraft model roll cues for the roll-only condition. However, due to the disabling of the specific force cancellation and the rotation around the motion reference point below the pilot, the roll motion resulted in large fluctuations in the lateral specific force (see Fig. 19a). In the sway-only condition, lateral specific forces were smaller and showed a better match with the aircraft model cues. Furthermore, in Fig. 19c the effect of the sway scaling factor $K_{f_y} = 0.6$ is visible for the sway-only condition. Note that the roll cues in this case originated from the tilt coordination, but since subthreshold tilting rates were used, the roll accelerations were negligible (see Fig. 19d). In the final case (the sway/roll/yaw condition), both sway and roll simulator cues roughly correlate with the aircraft cues, but here the effect of the extra scaling of the lateral filter gains is apparent (see Table 3).

In Fig. 20 the same simulator cues as in Fig. 19 are given in the frequency domain together with the sensory perception thresholds. It is shown that for the roll-only condition both sway specific forces and roll accelerations were superthreshold over a large frequency range. In the sway-only condition, the sway specific forces and roll acceleration were super- and subthreshold, respectively, as could be expected. Note that the perception of sway specific forces was assumed to be much less than in the roll-only case, which is an assumption supported by Fig. 19. Finally, both sway specific forces and roll acceleration are above threshold in the sway/roll/yaw condition. This analysis would indicate that different motion-cueing conditions can indeed influence motion perception and simulator fidelity. However, the combination of high workload and additional motion cues almost certainly increased the effective thresholds and

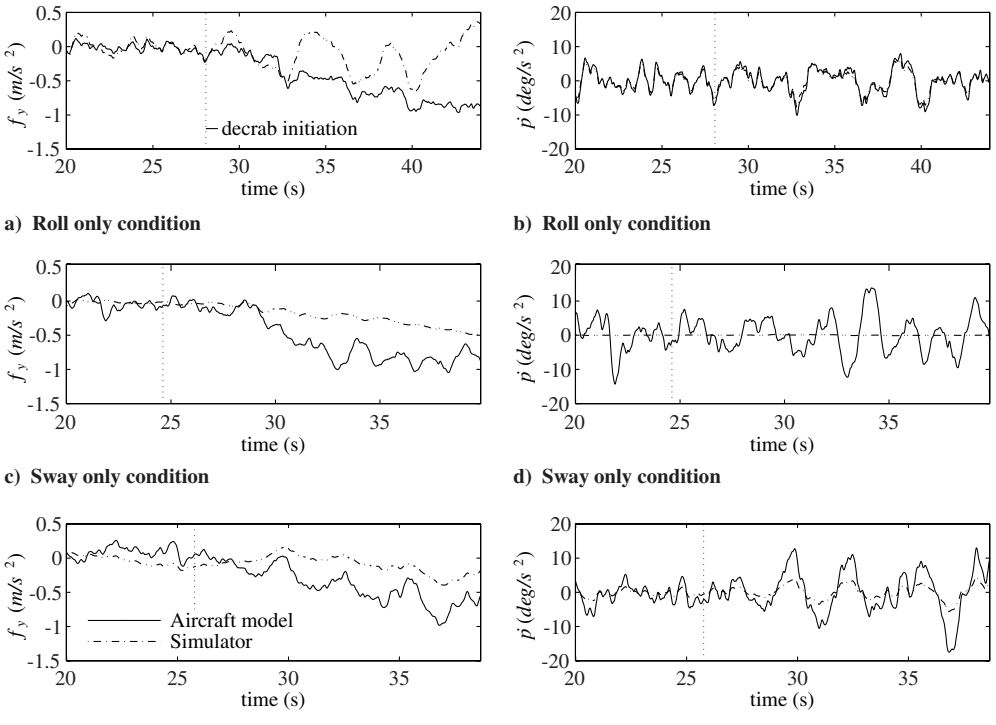

Fig. 19 Motion cues at pilot head in aircraft and simulator for different motion conditions.

pilots may still have had trouble distinguishing the different motions. Pilot comments indicate that these difficulties indeed occurred.

An overview of the statistical results for the decrab experiment is given in Table 8. On the basis of this overview, the implications of the results will be discussed. Furthermore, the subjective rating results will be compared with the results from earlier experiments by Groen et al. [29,30] and Smaili et al. [22].

A. Performance

Pilot performance metrics show little consistent variation over the different motion conditions. Only two main effects were significant: a decrease in lateral touchdown position in the presence of yaw and a decrease in RMS roll rate when roll was present. Yaw did not help significantly in reducing the lateral touchdown velocity or the heading alignment, which were the two other performance metrics that the pilots were briefed to minimize. It can therefore not be concluded from this data that the yaw motion (or any of the other motions for that matter) caused the pilot to perform his task better. Of course, the level of attained performance is not a measure of the simulator's fidelity or its usefulness for a particular task, and the pilots most certainly adapted to the different configurations to achieve a certain level of performance. The other main effect, a decrease in aircraft roll motions in the presence of simulator roll, coincides with some pilot comments that the simulator roll helped them minimize small pilot-induced roll oscillations. This effect is not, however, directly apparent in the RMS wheel rate, which would indicate that the motions were quite gentle.

In addition to these main effects, two significant interactions were found: vertical touchdown velocity between sway and yaw and maximum yaw rate between roll and yaw. The vertical velocity at touchdown decreased with the addition of sway motion when yaw was also present, but increased without yaw. The maximum yaw rate decreased with the addition of roll motion when yaw was also present, but increased without yaw.

B. Control Activity

No significant main effects were found for the examined pilot control variables. This is somewhat disappointing, since it was expected that the ability to employ pilot modeling techniques to differentiate between the motion conditions would initially be indicated by differences in the pilot control signals. So far, no modeling was successfully performed with the data for this experiment, and further studies are being planned.

The only significant effects were observed in the interaction between sway and yaw on the pedal deflection integrated over time within the decrab window and on the RMS of the control wheel deflection rate. The pedal deflection slightly decreased with the addition of sway when yaw was also present, but increased without yaw. The wheel rate exhibited the inverse behavior.

Table 8 Summary of the results of the decrab experiment

	Effects[a]						
Measure	y	r	s	r × y	s × y	s × r	s × r × y
			Performance				
Lat velocity td	——	MS	——	——	——	——	——
Lat position td	S	——	——	——	——	——	——
Heading alignment td	——	——	——	——	——	——	——
Vert velocity td	——	——	——	MS	S	MS	——
Long. position td	——	——	——	——	MS	——	——
RMS localizer error	——	——	——	——	——	——	——
RMS roll rate	——	S	——	——	——	——	——
Max yaw rate	MS	——	MS	S	——	——	——
Min crab angle	——	——	——	——	——	——	——
Decrab initiation	——	——	——	——	——	——	——
Avg decrab rate	——	——	——	——	——	——	——
			Control				
RMS pedal rate	MS	——	——	——	——	——	——
RMS wheel rate	——	——	——	——	S	——	——
Max pedal	——	MS	——	——	——	——	——
Integrated pedal	——	——	——	——	S	——	——

[a]S is significant ($p < 0.05$), MS is marginally significant ($p < 0.10$), and td denotes at touchdown.

Table 9 Comparison of rating results with studies of Groen et al. on GFORCE [29,30] and Smaili et al. on GRACE [22]

		Effects[a]					
Experiment	Subject[b]	y	r	s	r × y	s × y	s × r
			Motion perception				
GFORCE [29,30]	pnf	——	S	S	——	S	——
GRACE [22]	pnf	——	S	S	——	——	S
GRACE [22]	pf	——	S	——	——	S	——
SRS	pf	——	S[c]	S[d]	N/A	N/A	N/A
			Motion fidelity				
GFORCE [29,30]	pnf	S	S	——	——	——	——
GRACE [22]	pnf	——	——	S	——	——	S
GRACE [22]	pf	——	——	——	——	——	——
SRS	pf	——	——	——	——	——	——

[a]S is significant ($p < 0.05$), and MS is marginally significant ($p < 0.10$).
[b]Subject can be the pilot flying (pf) or pilot not flying (pnf).
[c]Roll-only condition is significantly larger than all others in pairwise comparison.
[d]Sway-only condition is significantly larger than no motion in pairwise comparison.

C. Ratings

Table 9 shows the results from the pilot ratings and compares them with the earlier studies introduced in Sec. III. As could be expected from the reported difficulties the participants had in discriminating the different motion conditions, no significant effects were found for the motion fidelity rating. The motion intensity perception rating was only examined in pairs showing a significant difference between the roll-only condition versus all others and the sway-only condition versus the no-motion condition. The relatively large lateral accelerations in the roll condition, which were caused by the distance between pilot head and the roll rotation axis and the absence of any mitigating lateral cues from the sway channel, are suspected to play an important role in this result.

These problems with subjective motion ratings, especially in combination with a relatively small number of participants, once again underline the desire to develop more objective metrics to investigate the influence of different motion components on pilot behavior. Although this study was not yet successful in applying such metrics, it is hoped that future studies can build on it to achieve this goal.

D. Reflection on Hypotheses

The first hypothesis was that sway motion would have a larger impact on performance and perceived motion than would roll or yaw. No significant effects of sway motion were found on any of the metrics, apart from an interaction with yaw on vertical velocity at touchdown. This hypothesis is therefore not supported by the data.

The second hypothesis was that sway and roll motion would increase the reported motion intensity. Although this is clearly the case for the roll-only condition, this is suspected to be a result of the implementation of this individual condition that led to large lateral specific forces at the pilot station. The addition of roll to any of the other conditions had no significant effect. The ratings are deemed to be not sufficient to support this hypothesis.

The third and final hypothesis was that yaw motion had no influence on any of the dependent measures. This was not the case, as yaw had a significant effect on lateral touchdown position and was involved in interactions on vertical velocity at touchdown and integrated pedal deflection (with sway) and on maximum yaw rate (with roll). This hypothesis must therefore be rejected.

VIII. Recommendations

In addition to the findings of the research described in this paper, some recommendations for future research can be put forward.

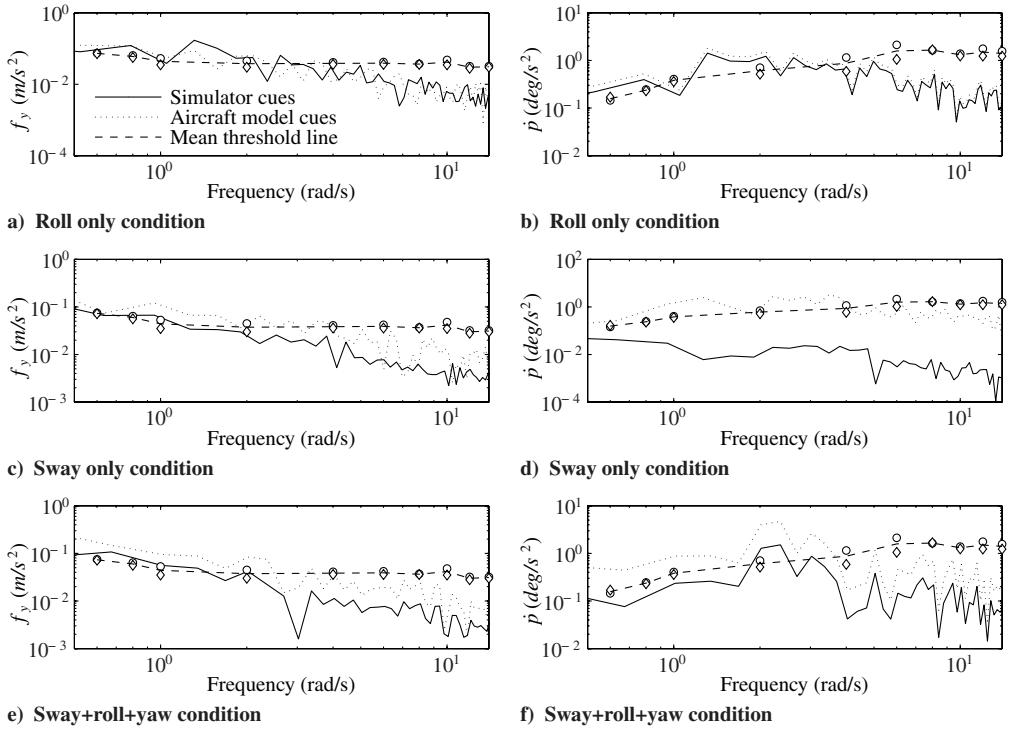

Fig. 20 Fourier transforms of sway specific forces and roll accelerations versus absolute perception thresholds [23].

The aircraft used in this research was relatively small compared with, for example, typical jet transport aircraft. Lateral motion profiles for decrab maneuvers will therefore be considerably different. As a subject for further research it is recommended to investigate the effects of aircraft size on the importance of motion cues in rotational and translational degrees of freedom.

In addition, further research into the roles of motion-cueing algorithm and motion-cueing strategy is proposed. Other motion-cueing algorithms are available that might increase the fidelity of lateral motion cueing during decrab maneuvers. Furthermore, the influence of motion-cueing strategy on performance and control results is of interest.

A validation study should be performed to compare decrab maneuvers performed in real flight by Delft University's Cessna Citation II aircraft with the data from this study to investigate the differences in pilot control behavior and aircraft response.

In the experiment simulation environment, a dynamic model for the horizontal interaction between aircraft landing gear and runway was not yet available. Lateral accelerations at touchdown due to a landing with high lateral velocity or a large heading alignment mismatch, which can adversely influence the control behavior of the pilots, were not perceivable in the simulator. The development of such a model is therefore recommended.

To improve the consistency and significance of the results, future studies should use more participants and see if improved training is necessary. In this study, the training used all motion configurations in random order, which perhaps prevented the pilots from developing an optimal piloting strategy for a particular motion configuration.

Ultimately, understanding the roles of simulator cues on pilot control behavior in transient maneuvers should result in the development of control-theoretical models for the description of pilot control in such maneuvers. With these models, the influence of simulator motion cues on pilot control behavior can be quantified, such that simulator fidelity can be evaluated more objectively. Future research will therefore focus on the modeling of pilot control behavior.

IX. Conclusions

A simulator experiment was performed to investigate the influence of different motion-cueing configurations on pilot performance, control, and perception during a decrab maneuver with a small business jet. The lateral motion cueing was varied over eight different configurations by enabling or disabling the lateral (yaw, sway, and roll) channels. The lateral filter gains were tuned to make full use of the available work space for each condition, and the longitudinal characteristics were kept constant.

Few significant results were found on both performance and control behavior, and virtually no significant effects were observed in the motion intensity and fidelity ratings. Participants reported having difficulty in consistently rating the motion cues during the short and high-workload decrab maneuver. A large variability was also observed between and within participants in how the decrab maneuver was performed, even though a consistent piloting strategy was strived for.

Results for the lateral motion-cueing degrees of freedom show that yaw motion had an unexpected significant effect on lateral touchdown position, but not on lateral touchdown velocity or longitudinal touchdown position or velocity. Sway motion had no significant effect on any of the performance or control metrics. Roll motion had a significant reducing effect on RMS aircraft roll rate, but not on the RMS wheel rate. Roll motion without accompanying sway or yaw motion led to relatively large lateral specific forces at the pilot station and was rated significantly more intense than any of the other configurations.

Appendix A: Reference Frames

As shown in Fig. A1, the origin of the aircraft's reference frames is located in the center of gravity. The body frame of reference (subscript b) is fixed to the aircraft and its X and Z axes lie in the plane of symmetry. The stability frame of reference (subscript s) is also fixed to the aircraft but additionally has its X axis aligned with the velocity vector in unperturbed flight.

The simulator's reference frames have their origin in the center of the circle through the upper gimbal points. The X axis lies in the vertical plane of symmetry and the Z axis points straight down. The inertial frame of reference (subscript i) remains fixed to the world with its origin in the upper gimbal points, whereas the actuators are extended to half their stroke. The simulator body frame of reference (subscript sim) moves with the simulator.

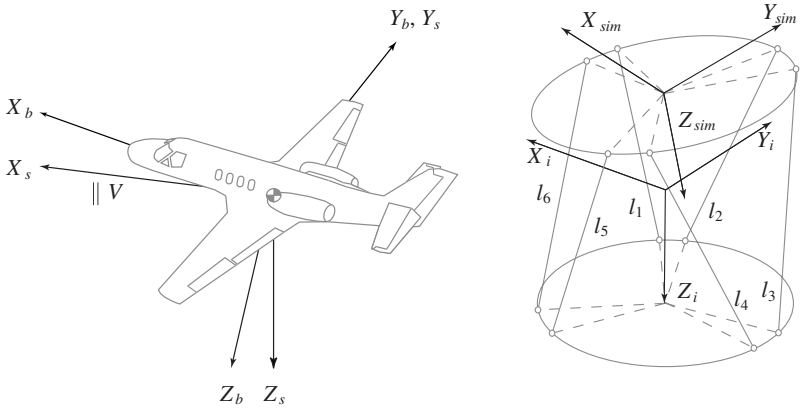

a) Aircraft reference frames

b) Simulator reference frames and actuator designations

Fig. A1 Definition of reference frames.

Acknowledgment

The authors would like to gratefully acknowledge the pilots who participated in the experiment described in this paper for their effort and useful comments.

References

[1] Hess, R. A., and Malsbury, T., "Closed-Loop Assessment of Flight Simulator Fidelity," *Journal of Aircraft*, Vol. 14, No. 1, March–July 1991, pp. 191–197. doi:10.2514/3.20621

[2] Hess, R. A., Malsbury, T., and Atencio, A., Jr., "Flight Simulator Fidelity Assessment in a Rotorcraft Lateral Translation Maneuver," *Journal of Guidance, Control, and Dynamics*, Vol. 16, No. 1, 1993, pp. 79–85. doi:10.2514/3.11430

[3] Zeyada, Y., and Hess, R. A., "Human Pilot Cue Utilization with Applications to Simulator Fidelity Assessment," *Journal of Aircraft*, Vol. 37, No. 4, 2000, pp. 588–597. doi:10.2514/2.2670

[4] Hess, R. A., and Siwakosit, W., "Assessment of Flight Simulator Fidelity in Multiaxis Tasks Including Visual Cue Quality," *Journal of Aircraft*, Vol. 38, No. 4, 2001, pp. 607–614. doi:10.2514/2.2836

[5] Zeyada, Y., and Hess, R. A., "Computer-Aided Asessment of Flight Simulator Fidelity," *Journal of Aircraft*, Vol. 40, No. 1, 2003, pp. 173–180. doi:10.2514/2.3072

[6] Groen, E. L., Smaïli, M. H., and Hosman, R. J. A. W., "Simulated Decrab Maneuver: Evaluation with a Pilot Perception Model," AIAA Modeling and Simulation Technologies Conference and Exhibit, San Francisco, AIAA Paper 2005-6108, 2005.

[7] Zaychik, K. B., Cardullo, F. M., and George, G., "A Conspectus on Operator Modeling: Past, Present and Future," AIAA Modeling and Simulation Technologies Conference and Exhibit, Keystone, CO, AIAA Paper 2006-6625, 2006.

[8] Hess, R. A., and Marchesi, F., "Pilot Modeling with Applications to the Analytical Assessment of Flight Simulator Fidelity," AIAA Modeling and Simulation Technologies Conference and Exhibit, Honolulu, HI, AIAA Paper 2008-6682, 2008.

[9] Hosman, R., van der Geest, P., and van der Zee, J., "Development of a Pilot Model for the Manual Balked Landing Maneuver," AIAA Modeling and Simulation Technologies Conference and Exhibit, Chicago, AIAA Paper 2009-5818, 2009.

[10] Van den Berg, P., Zaal, P. M. T., Mulder, M., and Van Paassen, M. M., "Preparation for Conducting Multi-Modal Pilot Model Identification in Real Flight," AIAA Modeling and Simulation Technologies Conference and Exhibit, Keystone, CO, AIAA Paper 2006-6630, 2006.

[11] Mulder, M., and Mulder, J. A., "Cybernetic Analysis of Perspective Flight-Path Display Dimensions," *Journal of Guidance, Control, and Dynamics*, Vol. 28, No. 3, 2005, pp. 398–411. doi:10.2514/1.6646

[12] Steurs, M., Mulder, M., and Van Paassen, M. M., "A Cybernetic Approach to Assess Flight Simulator Fidelity," AIAA Modelling and Simulation Technologies Conference and Exhibit, Providence, RI, AIAA Paper 2004-5442, 2004.

[13] Zaal, P. M. T., Pool, D. M., Mulder, M., Van Paassen, M. M., and Mulder, J. A., "Identification of Multimodal Pilot Control Behavior in Real Flight," *Journal of Guidance, Control, and Dynamics* (to be published).

[14] Ellerbroek, J., Stroosma, O., Mulder, M., and Van Paassen, M., "Role Identification of Yaw and Sway Motion in Helicopter Yaw Control Tasks," *Journal of Aircraft*, Vol. 45, No. 4, July–Aug. 2008, pp. 1275–1289. doi:10.2514/1.34513

[15] Zaal, P. M. T., Pool, D. M., Mulder, M., and Van Paassen, M. M., "Multimodal Pilot Control Behavior in Combined Target-Following Disturbance-Rejection Tasks," *Journal of Guidance, Control, and Dynamics*, Vol. 32, No. 5, 2009, pp. 1418–1428. doi:10.2514/1.44648

[16] Pool, D. M., Zaal, P. M. T., Damveld, H. J., Van Paassen, M. M., and Mulder, M., "Pilot Equalization in Manual Control of Aircraft Dynamics," *2009 IEEE International Conference on Systems, Man & Cybernetics*, Inst. of Electrical and Electronics Engineers, Piscataway, NJ, 2009, pp. 2554–2559.

[17] Pool, D. M., Zaal, P.M. T., Van Paassen, M. M., and Mulder, M., "Effects of Heave Washout Settings in Aircraft Pitch Disturbance Rejection," *Journal of Guidance, Control, and Dynamics*, Vol. 33, No. 1, 2010, pp. 29–41. doi:10.2514/1.46351

[18] Zaal, P. M. T., Pool, D. M., De Bruin, J., Mulder, M., and Van Paassen, M. M., "Use of Pitch and Heave Motion Cues in a Pitch Control Task," *Journal of Guidance, Control, and Dynamics*, Vol. 32, No. 2, 2009, pp. 366–377. doi:10.2514/1.39953

[19] Van Paassen, M. M., and Mulder, M., "Identification of Human Control Behavior," *W. Karwowski: International Encyclopedia of Ergonomics and Human Factors*, 2nd ed., Taylor & Francis, London, 2006, pp. 400–407.

[20] Nieuwenhuizen, F. M., Zaal, P. M. T., Mulder, M., van Paassen, M. M., and Mulder, J. A., "Modeling Human Multichannel Perception and Control Using Linear Time-Invariant Models," *Journal of Guidance, Control, and Dynamics*, Vol. 31, No. 4, 2008, pp. 999–1013. doi:10.2514/1.32307

[21] Zaal, P. M. T., Pool, D. M., Chu, Q. P., van Paassen, M. M., Mulder, M., and Mulder, J. A., "Modeling Human Multimodal Perception and Control Using Genetic Maximum Likelihood Estimation," *Journal of Guidance, Control, and Dynamics*, Vol. 32, No. 4, 2009, pp. 1089–1099. doi:10.2514/1.42843

[22] Smaili, M. H., Jansen, H., Naseri, A., Groen, E. L., and Stroosma, O., "Pilot Motion Perception and Control During a Simulated Decrab Maneuver," AIAA Modeling and Simulation Technologies Conference and Exhibit, Hilton Head, SC, AIAA Paper 2007-6797, 20–23 Aug. 2007.

[23] Heerspink, H. M., Berkouwer, W. R., Stroosma, O., Van Paassen, M. M., Mulder, M., and Mulder, J. A., "Evaluation of Vestibular Thresholds for Motion Detection in the SIMONA Research Simulator," AIAA Modeling and Simulation Technologies Conference, AIAA Paper 2005-6502, 2005.

[24] Valente Pais, A. R., Mulder, M., Van Paassen, M. M., Wentink, M., and Groen, E. L., "Modeling Human Perceptual Thresholds in Self-Motion Perception," AIAA Modeling and Simulation Technologies Conference and Exhibit, Keystone, CO, AIAA Paper 2006-6626, 2006.

[25] Pool, D. M., Mulder, M., Van Paassen, M. M., and Van der Vaart, J. C., "Effects of Peripheral Visual and Physical Motion Cues in Roll-Axis Tracking Tasks," *Journal of Guidance, Control, and Dynamics*, Vol. 31, No. 6, 2008, pp. 1608–1622. doi:10.2514/1.36334

[26] Reid, L. D., and Nahon, M. A., "Flight Simulation Motion-Base Drive Algorithms: Part 3. Pilot Evaluations," Univ. of Toronto Inst. for Aerospace Studies TR 319, Dec. 1986.

[27] Schroeder, J. A., "Helicopter Flight Simulation Motion Platform Requirements," NASA TR TP-1999-208766, July 1999.

[28] Grant, P. R., Yam, B., Hosman, R. J. A. W., and Schroeder, J. A., "Effect of Simulator Motion on Pilot Behavior and Perception," *Journal of Aircraft*, Vol. 43, No. 6, Nov.–Dec. 2006, pp. 1914–1924. doi:10.2514/1.21900

[29] Groen, E. L., Smaili, M. H., and Hosman, R. J. A. W., "Simulated Decrab Maneuver: Evaluation with a Pilot Perception Model," AIAA Modeling and Simulation Technologies Conference and Exhibit, San Francisco, AIAA Paper 2005-6108, 15–18 Aug. 2005.

[30] Groen, E. L., Hosman, R. J. A. W., and Smaili, M. H., "Perception Model Analysis of Flight Simulator Motion for a Decrab Maneuver," *Journal of Aircraft*, Vol. 44, No. 2, 2007, pp. 427–435. doi:10.2514/1.22872

[31] Schmidt, S. F., and Conrad, B., "Motion Drive Signals for Piloted Flight Simulators," NASA TR CR-1601, May 1970.

[32] Reid, L. D., and Nahon, M. A., "Flight Simulation Motion-Base Drive Algorithms: Part 1. Developing and Testing the Equations," Univ. of Toronto Inst. for Aerospace Studies TR 296, Dec. 1985.

[33] Reid, L. D., and Nahon, M. A., "Flight Simulation Motion-Base Drive Algorithms: Part 2. Selecting the System Parameters," Univ. of Toronto Inst. for Aerospace Studies TR 307, May 1986.

[34] Hosman, R. J. A. W., "Pilot's perception and control of aircraft motions," Ph.D. Thesis, Faculty of Aerospace Engineering, Delft Univ. of Technology, Delft, The Netherlands, 1996.

[35] Beukers, J. T., Stroosma, O., Pool, D. M., Mulder, M., and Van Paassen, M. M., "Investigation of Pilot Perception and Control During Decrab Maneuvers in Simulated Flight," AIAA Modeling and Simulation Technologies Conference and Exhibit, Chicago, AIAA Paper 2009-6030, 2009.

[36] Grant, P. R., and Reid, L. D., "Motion Washout Filter Tuning: Rules and Requirements," *Journal of Aircraft*, Vol. 34, No. 2, 1997, pp. 145–151. doi:10.2514/2.2158

[37] Gouverneur, B., Mulder, J. A., Van Paassen, M. M., Stroosma, O., and Field, E. J., "Optimisation of the SIMONA Research Simulator's Motion Filter Settings for Handling Qualities Experiments," AIAA Modeling and Simulation Technologies Conference and Exhibit, Austin, TX, AIAA Paper 2003-5679, 11–14 Aug. 2003.

[38] Sinacori, J. B., "The Determination of Some Requirements for a Helicopter Flight Simulator Facility," NASA TR CR-152066, 1977.

[39] Stroosma, O., Van Paassen, M. M., and Mulder, M., "Using the SIMONA Research Simulator for Human-Machine Interaction Research," AIAA Modeling and Simulation Technologies Conference and Exhibit, Austin, TX, AIAA Paper 2003-5525, 11–14 Aug. 2003.

[40] Berkouwer, W. R., Stroosma, O., Van Paassen, M. M., Mulder, M., and Mulder, J. A., "Measuring the Performance of the SIMONA Research Simulator's Motion System," AIAA Modeling and Simulation Technologies Conference and Exhibit, San Francisco, AIAA Paper 2005-6504, 2005.

[41] Van de Moesdijk, G. A. J., "Simulation of Patchy Atmospheric Turbulence, Based on Measurements of Actual Turbulence," Memo. M-240, Delft Univ. of Technology, Delft, The Netherlands, Oct. 1975.

[42] Van der Linden, C. A. A. M., "DASMAT: the Delft University Aircraft Simulation Model and Analysis Tool," Delft Univ. of Technology TR LR-781, Delft, The Netherlands, 1996.